INVESTIGATING THE DISTRIBUTION OF FROSTS IN RELATION TO PRESENT-DAY GULLY ACTIVITY ON MARS.

A. R. Khuller[1], P. R. Christensen[1], T. N. Harrison[1] and S. Diniega[2], [1]Arizona State University, Tempe, AZ, USA (akhuller@asu.edu), [2] Jet Propulsion Laboratory, California Institute of Technology, Pasadena, CA, USA.

Introduction: A wide range of types of activity in mid-latitude Martian gullies has been observed over the last decade [1-7], with some activity constrained temporally to occur in the coldest times of year (winter and spring; [2-8]), suggesting that surficial frosts that form seasonally and diurnally might play a key role in this present-day activity. Frost formation is highly dependent on two key factors: (1) surface crystal temperature and (2) atmospheric partial pressure of the condensable gas [9]. Since the Martian atmosphere is primarily composed of CO_2, surficial frost formation is not diffusion-limited (unlike H_2O) [10].

Hence, for temperatures exceeding the local frost point of CO_2, (~ 148 K at a surface pressure of 610 Pa) frost is always present [10]. Typically, the contents of these frosts are dominated volumetrically by CO_2, although small amounts of H_2O frosts are also present, and typically precede CO_2 frost deposition (due to water's higher condensation temperature [11]).

Here we use the Thermal Emission Imaging System (THEMIS) and the Thermal Emission Spectrometer (TES) onboard Mars Odyssey and Mars Global Surveyor, respectively, to explore the global spatial, temporal variation of temperatures conducive to CO_2, H_2O frost formation on Mars and assess their distribution with gully landforms.

Methods: THEMIS (~100 m/pixel) has a single-pixel noise equivalent spectral radiance (NESR) of 2.72×10^{-6} W cm^{-2} sr^{-1} μm^{-1} in band 9, corresponding to a 1-σ noise equivalent delta temperature (NEDT) of ~0.4 K at 245 K; and 1.1 K at 180 K [12]. Using this NESR, the NEDT for CO_2 frost formation temperatures can be calculated [13]. From Fig. 1, it can be seen that at 130 K, the NEDT is 7 K whereas at 154 K it is ~2.5 K. TES (~3 km/pixel) has an absolute accuracy of 4×10^{-8} W cm^{-2} sr^{-1} cm^{-1}, corresponding to an absolute temperature error of ~0.4 K at 280 K and ~1.5 K at 150 K [14].

Each THEMIS image is divided into framelets that are ~ 32 km wide, with varying lengths [15]. THEMIS surface brightness temperature is archived at the framelet level [15] and was queried using a PSQL-based query scheme in Davinci (http://davinci.asu.edu). Temperatures of the center pixel of each framelet were queried; temperatures are derived from Band 9 (centered at 12.57 μm) THEMIS data [12]. Temperatures of 130-154 K were noted, as this is the approximate range of the global CO_2 frost point. Systematic noise was removed by excluding framelets with calibration errors and dropouts.

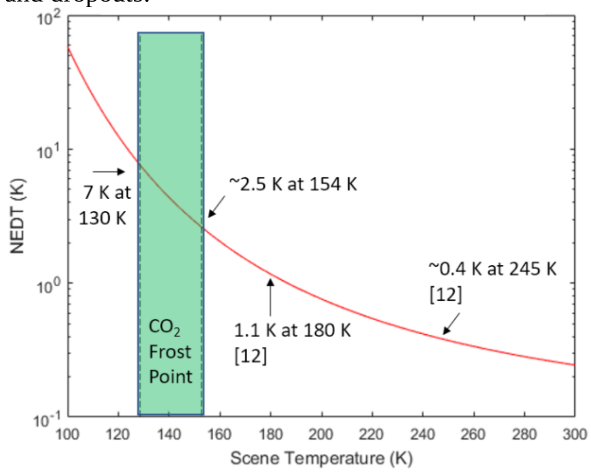

Figure 1. *THEMIS band 9 Noise Equivalent Delta Temperature (NEDT) vs. scene temperature. The global temperature range of the CO_2 frost point is highlighted in green.*

TES water vapor column abundance data [16] was used to calculate the likely H_2O frost point for Martian Year (MY) 26, assuming a constant surface pressure of 600 Pa and a well-mixed atmosphere.

Results: Consistent with previous coarser resolution thermal data (e.g. [10]), it is apparent that temperatures conducive to the presence of CO_2 frost are pervasive across all latitudes (Fig. 2).

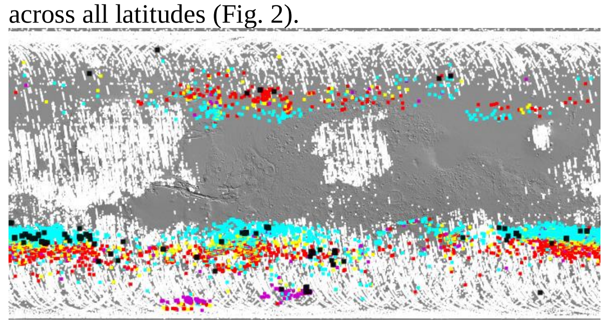

Figure 2. *THEMIS framelet center pixels (130-154 K; white) with gully distribution (blue = poleward-facing, yellow = east/west, red = equatorward, purple = no preference; [7]) and active gullies (black; [4]).*

Frost temperatures are confined to low thermal inertia regions [17] within latitudes closer to the equator (Fig. 3), with frosts there occurring diurnally and seasonally [10].

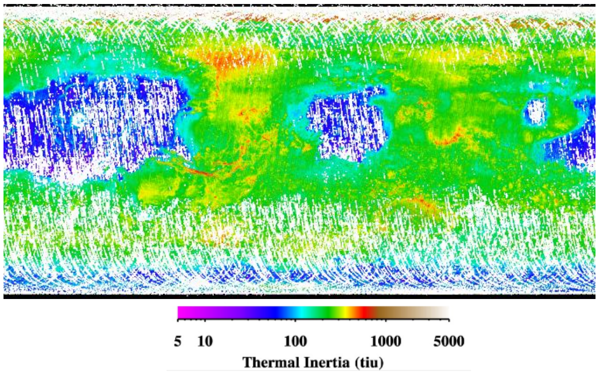

Figure 3. *THEMIS 130-154 K framelet center pixels (white) overlaid on TES nighttime thermal inertia [17].*

In the southern hemisphere, the extent of observed and active gullies [4, 7] is contained within the extent of frost framelets (Fig. 2). In the northern hemisphere, most gullies are present in regions where framelets without the frost temperature are observed. H_2O frost temperatures derived from daytime TES data (Fig. 4) match well with in-situ measurements made by the Phoenix lander at 68.22N, from L_s 78º-148º (194-206 K; [18]).

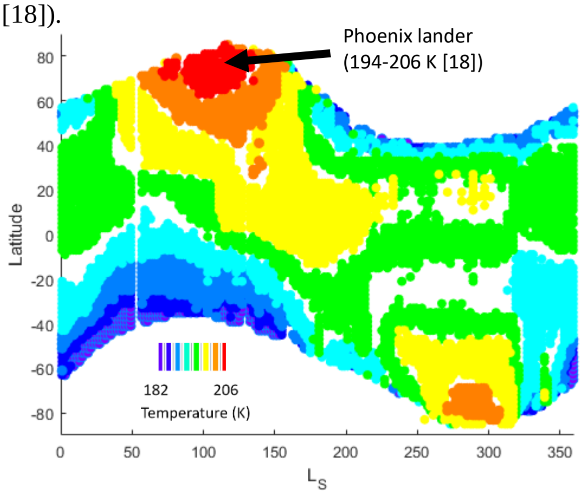

Figure 4. *Seasonal (MY = 26) variation of H_2O frost temperature derived from TES water vapor column abundance [16].*

Discussion: Gullies are especially active in sand dunes [8], with smaller-scale changes (relative to the entire gully) observed in other loose, unconsolidated substrates downslope or within existing gully alcoves [4, 6]. Present-day gully activity has been attributed to frost (primarily CO_2, with relatively minor amounts of H_2O) sublimation-induced flows; some authors (e.g. [4]) argue that the nature of this activity represents the formation of most gullies. Frost-induced gully activity can lead to increased frost formation within existing gullies (i.e., within topographically shadowed gully alcoves, channels, etc.), resulting in a positive feedback system between gullies and frosts. Although the amounts of frost will vary with latitude, CO_2 frosts are likely to be present at all latitudes (Figs. 2, 3). However, it is possible that CO_2 frosts at the sub-pixel level (micro-climates within topographically shadowed alcoves, etc. can be key to gully formation/evolution) are not accounted for in this global, THEMIS framelet-scale study. Additionally, the THEMIS NEDT present near CO_2 frost temperatures can lead to non-detections.

If gullies are formed primarily by CO_2 frost mechanisms, one would expect some correlation with the observance of CO_2 frost temperatures and gully distribution (where slopes are available). Although there exist a few poorly developed, mass-wasting morphologies near the equator [19], most gullies (including those found to be active in the present-day) are found poleward of 30° in both hemispheres. H_2O frost temperatures (Fig. 4) are readily attained near the equator [20], and can perhaps explain some present-day mass-wasting activity. The lack of correlation of northern hemisphere gullies with frosts has been attributed to climate cycling caused by changes in orbital parameters over time [4].

Based on seasonal constraints on gully activity timing, frost presence from visible imagery [4-6, 8], spectral data [21] and thermal data (this work), it is likely that most present-day activity can be explained by frosts. However, whether or not present-day gully activity is representative of gully formation as a whole is still open to debate, with details on CO_2 frost-induced gully formation mechanisms still unresolved.

References: [1] Malin M.C. et al. (2006) *Science, 314*, 1573-1577. [2] Harrison T.N. et al. (2009) *DPS 41*, Abstract #41. [3] Dundas C. M. et al. (2010) *GRL, 37*, 7. [4] Dundas C. M. et al. (2017) *GSL*, 467, SP467-5. [5] Dundas C. M. et al. (2012) *Icarus, 220, 124-143.* [6] Dundas C. M. et al. (2015) *Icarus, 251*, 244-263. [7] Harrison T.N. et al. (2015) *Icarus, 252*, 236-254. [8] Diniega S. et al. (2018) *LPI*, Abstract #2086. [9] Kieffer H.H. (1968) *Diss.* [10] Piqueux S. et al. (2016) *JGR, 121*, 1174–1189. [11] Schorghofer N. and Edgett K.S. (2006) *Icarus, 180, 3*21-334. [12] Christensen P. R. et al. (2003) *Science, 300*, 2056-2061. [13] Cao C. and Shao X. (2018) [14] Christensen P. R. et al. (2001) *JGR, 106*, 23823-23871. [15] Murray K. (2009). [16] Smith M. D. (2002) *JGR, 107*, 25-1. [17] Putzig N. E. and Mellon M. T. (2007) *Icarus, 191*, 68-94. [18] Zent A. P. et al. (2016) *JGR, 121*, 626-651. [19] McEwen A. S. et al. (2018) *EPSC, 17*, 21. [20] Landis G. A. (2007) LPS XXXVIII, Abstract #2423. [21] Vincendon M. et al. (2015) J*GR, 120*, 1859-1879.

Acknowledgements: ARK would like to thank K. Murray, S. Piqueux, H. H. Kieffer, A. Lal, S. Dickenshied, M. Burris and M.D. Smith for very helpful discussions. ARK acknowledges the support of the Barrett Bidstrup and R. Greeley Scholarships for this work.